

Picosecond Solvation Dynamics of Coumarin153 in Bis(1-methyl-1H-imidazol-3-ium-3-yl)dihydroborate Cation Containing Room Temperature Ionic Liquid and Ionic Liquid-DMF Mixtures

Prabhat Kumar Sahu, Sudhir Kumar Das and Moloy Sarkar*

School of Chemical Sciences, National Institute of Science Education and Research, Bhubaneswar 751005, Orissa, India

Abstract: Steady state and time-resolved fluorescence behavior of coumarin153(C153) in bis(1-methyl-1H-imidazol-3-ium-3-yl)dihydroborate cation containing room temperature ionic liquid and its mixture with dimethylformamide (DMF) has been investigated. Density functional calculations on the present ionic liquid have been carried out to have ground state structural information of this system. C-H...N and C-H...O hydrogen bonding interactions between cationic and anionic moiety of the present ionic liquid has been observed. Steady state absorption and emission spectral profiles of C153 are found not to be influenced by the polar cosolvent. Time-resolved fluorescence anisotropy experiments show that the rotational motion of the probe becomes faster in presence of DMF. During time dependent dynamic Stokes shift measurements in ionic liquid-DMF mixtures, the average solvation time is found to decrease with the addition of DMF to the ionic liquid. The decrease in both average solvation and rotational time of probe molecule upon gradual addition of polar organic co-solvent is attributed to the lowering of bulk viscosity of the medium.

Keywords: Ionic liquid, Time-dependent Stokes shift, Solvation dynamics, polar cosolvent, Anisotropy.

INTRODUCTION

In recent years, room-temperature ionic liquids (RTILs) have drawn great attention due to its versatile applications in the fields of chemical, material and biological sciences [1, 2]. Curiosity about their structure – property correlations have also motivated many researchers to carry out experimental and theoretical studies on these systems [3-13]. However, many of the studies have been carried out by taking neat room temperature ionic liquid as the medium. Interestingly, over the past few years, mixed ionic liquid-cosolvent systems are found to be extremely useful in several new applications, such as organic synthesis [14], catalysis [15], polymerization processes [16], extraction of solutes from solvent [17, 18] etc. Keeping in mind the uses of RTIL-cosolvent systems in new potential applications, it is of paramount importance to have thorough understanding of the roles of cosolvents that they play in governing the properties of RTILs.

Some studies have been carried out to understand the physicochemical properties of the RTILs-cosolvents mixtures [19-26]. It has been found out that viscosity [19], polarity [20-22], solvation [23, 24] and electrochemical [25, 26] behavior of the ionic liquid undergo perceptible changes in presence of cosolvents. Since solute reactivity is intricately related to solvation dynamics, studies on dynamics of solvation

by monitoring the time-dependent fluorescence Stokes shift (TDFSS) of a dipolar solute in the given medium [6, 8-11] have been carried out to understand the dynamical features of IL-cosolvent mixtures. In this regard Paul *et al.* [6] have studied the effect of nonpolar toluene and dioxane on the solvation dynamics and solute rotation in 1-butyl-3-methylimidazolium hexafluorophate. The composition dependence of Stokes shift dynamics of a fluorescent dye molecule in IL-cosolvent mixtures has been investigated theoretically by Ranjit Biswas *et al.* [12]. The theory demonstrates the dynamic Stokes shift as a sum of contributions from the dye-RTIL and the dye-polar cosolvent interactions. The theory also suggests significant contribution from solute-cation dipole-dipole interaction in solvation energy relaxation. Moreover, Stokes shift dynamics in ([Bmim][BF₄]+ dichloromethane) binary mixtures predicts a very weak nonlinear composition dependence.

In this context, it may be mentioned that Sarkar and coworkers' [8-11] have studied the effects of polar solvents such as, acetonitrile, water and methanol on the dynamics of solvation of ammonium and imidazolium-based ionic liquids. These studies have demonstrated that addition of cosolvents in RTILs affects both the solvent relaxation as well as solute rotation. Very recently, we have also investigated the solvation and rotational relaxation behavior of a dipolar probe in ultra hydrophobic 1-(2-Methoxyethyl)-1-methylpyrrolidinium tris(pentafluorethyl)trifluorophosphate and its mixture with toluene [13]. It has been observed that toluene can effectively penetrate into the

*Address correspondence to this author at the School of Chemical Sciences, National Institute of Science Education and Research, Bhubaneswar 751005, Orissa, India; Tel: +91-674-2304037; Fax: +91-674-2304050; E-mail: moloy.sarkar@gmail.com

ionic liquid-rich cybotactic region of the probe. This has been explained by considering favorable noncovalent interaction between ionic liquid and toluene. One general observation of the TDFSS studies is that the addition of a cosolvent to ionic liquid decreases the average solvation time and rotational time of the probe due to the lowering of viscosity of the media.

Dimethylformamide (DMF) is an interesting solvent with a strong electron-pair donating and accepting ability. It has been used to dissolve a wide range of organic and inorganic compounds which in turn has also made this solvent to be used in variety of industrial processes [27-29]. Moreover, it has been widely used in developing solvent reactivity relationships [30-32]. In view of this, it is expected that the RTIL-DMF will serve as an excellent solvent system for several applications. Very recently, Anil Kumar and coworkers have studied the thermophysical properties of binary mixtures of DMF with ammonium and imidazolium based ionic liquids [33]. However, to the best of our knowledge there is no report of solvent and rotational relaxation studies by taking DMF as cosolvent for RTILs. We would also like to take a note here that, RTIL-cosolvent systems are known to be micro-heterogeneous [34-37]. In this regard, it would also be an interesting study to find a relationship between average solvation and rotational time and medium viscosity.

Keeping all these in mind, we have investigated the solvation and rotational relaxation of Coumarin153 (C153) in Bis(1-methyl-1H-imidazol-3-ium-3-yl)dihydroborate bis(trifluoromethylsulfonyl)amide and RTIL-DMF mixtures. The present RTIL is an interesting one in a sense that two methylimidazolium cationic moieties are bridged by a borohydride group and the cationic charge is compensated by NTf_2^- . In all previous cases, solvation and rotational dynamics were studied using monocationic imidazolium moiety. The probe C153 used in the present study is a well-known solvatochromic probe suitable for dynamic Stokes shift

measurements [38]. The molecular diagram of RTIL and C153 are shown in Figure 1.

EXPERIMENTAL SECTION

Materials

C153 (laser grade, Exciton) was used as received. The ionic liquid was obtained from Frontier Scientific Chemicals, USA (95% purity) and purity of IL was confirmed from ^1H NMR spectrum. The IL was kept in high vacuum at $60^\circ\text{--}70^\circ\text{C}$ for one day to remove any moisture present in this solvent. The IL was taken in a long-necked quartz cuvette and requisite amount of fluorophore was added to prepare the solution. Proper precaution was taken to avoid moisture absorption by the media during transferring the solute into the cuvette. During measurements, the concentration of the dye molecule (C153) was kept low so as to prevent dye aggregation.

Instrumentation

The viscosity of the RTIL was measured by LVDV-III Ultra Brookfield Cone and Plate viscometer (1% accuracy and 0.2% repeatability). ^1H NMR spectra were obtained on a Spectrometer Bruker AVANCE 400 NMR Spectrometer at ambient temperature using tetramethylsilane (TMS) as an internal standard. ^1H -NMR (DMSO-d_6 , 400 MHz): δ (ppm) = 8.65 (s, 2H), 7.51 (m, 2H), 7.35 (m, 2H), 3.79(s, 6H). The steady state absorption spectra were recorded on Perkin Elmer, Lambda-750 UV/VIS spectrophotometer and fluorescence spectra were recorded on a Perkin Elmer, LS 55 spectrofluorimeter. Time-resolved fluorescence measurements were carried out using a time-correlated single-photon counting (TCSPC) spectrometer (Edinburgh, OB920). Diode laser ($\lambda_{\text{exc}} = 405$ nm, FWHM = 98 ps) was used to excite the probe, and an MCP photomultiplier (Hamamatsu R3809U-50) was used as the detector (response time 40 ps). The excitation source profile was recorded by scatterer

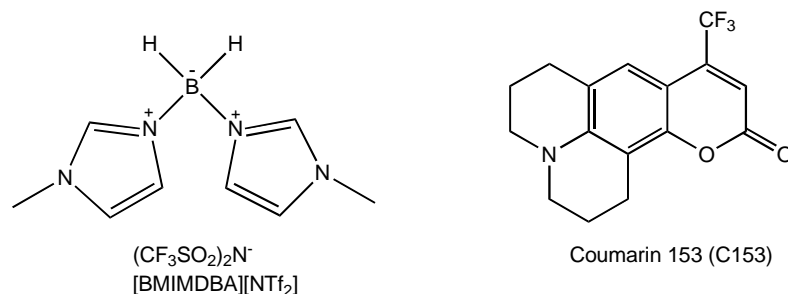


Figure 1: Molecular Structures of Bis(1-methyl-1H-imidazol-3-ium-3-yl)dihydroborate bis(trifluoromethylsulfonyl)amide [BMIMDBA][NTf₂] and Coumarin153 (C153).

(dilute ludox solution in water) in place of the sample. The temperature was controlled by the Quantum Northwest (TC125) instrument. Decay curves were analyzed by nonlinear least-squares iteration procedure using F900 decay analysis software. The quality of the fit was judged by the chi square (χ^2) values and weighted deviation was obtained by fitting. The time-resolved fluorescence anisotropy measurement was done by using two polarizer by placing one of them in the excitation beam path and the other one in front of the detector. An alternate collection of the fluorescence intensity in parallel and perpendicular polarization (with respect to the vertically polarized excitation laser beam) for equal interval of time had been carried out until the count difference between the two polarizations (at $t = 0$) is ~ 5000 . For G-factor calculation, the same procedure was adopted, but with 5 cycles and horizontal polarization of the exciting laser beam.

Method

The time resolved emission decay profile were measured at 5/10 nm intervals around the whole emission spectra. The total number of measurements was 25-35 in each case. In all cases, when decay was monitored at a shorter wavelength, a faster decay was observed, and at a longer wavelength, we observed a decay profile that consists clear rise with usual decay. Each decay curve was fitted to a triexponential decay function with an iterative reconvolution program (F900) maintaining the χ^2 between 1 and 1.2 as a measure of goodness of fit. The time resolved emission spectra (TRES) were constructed according to a procedure described earlier [13].

The emission maximum at each time $\bar{\nu}(t)$ was obtained by fitting the spectrum to a log-normal line-shape function as given below

$$I = h \exp[-\ln 2 \{ \ln(1+\alpha) / \gamma \}^2] \quad (1)$$

for $\alpha > -1$ and $I = 0$ for $\alpha \leq -1$

where $\alpha = 2\gamma (\bar{\nu} - \bar{\nu}_{peak}) / \Delta$, $\bar{\nu}_{peak}$ was the wavenumber corresponding to the peak, h was the peak height, Δ was the full width at half maximum (FWHM) and γ was a measure of the asymmetry of the band shape. Optimizing these four parameters by nonlinear least squares iteration, the best fitted curve was obtained. The peak frequencies were obtained from this log-normal fitting of TRES. The peak frequencies were then used to construct the solvent correlation function ($C(t)$).

$$C(t) = \frac{\bar{\nu}(t) - \bar{\nu}(\infty)}{\bar{\nu}(0) - \bar{\nu}(\infty)} \quad (2)$$

where $\bar{\nu}(0)$ was the peak frequency at time $t = 0$, just after the electronic excitation and $\bar{\nu}(t)$ was the peak frequency at time $t = t$. Again, $\bar{\nu}(\infty)$ was the peak frequencies at $t = \infty$ when solvent molecules were in the equilibrium position around the photoexcited probe molecule. The time dependence of the calculated $C(t)$ was fitted by a biexponential function of the form

$$C(t) = a_1 e^{-t/\tau_1} + a_2 e^{-t/\tau_2} \quad (3)$$

where τ_1 and τ_2 are the solvent relaxation times and a_1 and a_2 were normalized pre-exponential factors. After having the values of τ_1 , τ_2 and a_1 , a_2 , the average solvation time was calculated by using the following relation

$$\langle \tau_{solv.} \rangle = a_1 \tau_1 + a_2 \tau_2 \quad (4)$$

We have also fitted $C(t)$ by the stretched exponential function as given below.

$$C(t) = \exp(-(t/\tau_{solv})^\beta) \quad (5)$$

Where $0 < \beta \leq 1$

$$\langle \tau_{st} \rangle = \frac{\tau_{solv}}{\beta} \Gamma(\beta^{-1}) \quad (6)$$

where Γ was the gamma function and τ_{st} was the average solvation time considering $C(t)$ was a stretched exponential function.

RESULTS AND DISCUSSION

Optimized Structure

To know the structural features of [BIMIMDBA][TF₂N] we have optimized the structure of this IL in the ground state with B3LYP functional [39, 40] and 6-31++G (d, p) basis set using Gaussian 3.0 program [41]. The optimized structure of [BIMIMDBA][TF₂N] is shown in Figure 2. The van der Waals criterion for hydrogen bond formation is that for the formation of X—H...Z bonds, the distance between X...Z should be less than the sum of the X—H covalent bond and the van der Waals radii of H and Z [42]. The van der Waals radii of O, N and H are 1.52 Å, 1.55 Å and 1.2 Å respectively. In the optimized structure, the distance between O33—H17, O34—H4 and N28—H17 are measured to be 2.614 Å, 2.172 Å and 2.451 Å respectively (Figure 2). Moreover, the bond angles

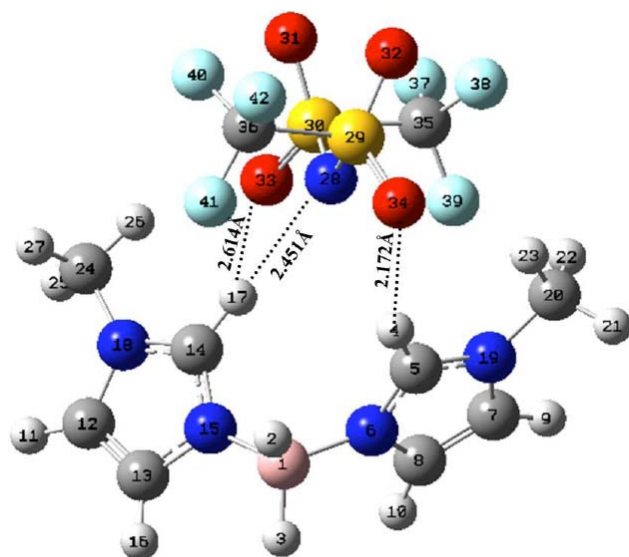


Figure 2: Optimized structure of [BIMIMDBA][TF₂N].

C14–H17–N28, C14–H17–O33 and C5–H4–O34 are found to be 179.4°, 122.3° and 141.3° respectively. In the present case, these calculated data of both the distance and the angle suggests the presence of strong C–H···N hydrogen bonding interactions between the cationic and the anionic fragment of the RTIL. The data also depicts a weak C–H···O interaction between the cationic and the anionic moiety. The structural parameters as obtained from the gas phase optimized structure of the present ionic liquid are collected in Table 1.

Steady State Behavior

The absorption and emission spectra of C153 are recorded both in neat RTIL and RTIL-DMF mixture.

The absorption and emission maxima of C153 in neat ionic liquid and its binary mixture with DMF are shown in Table 2. The representative steady state emission spectra of C153 in neat RTIL and RTIL-DMF binary mixtures are also shown in Figure 3. In the present case, no significant emission from the ionic liquid has been observed; the fact has enabled us to use the present ionic liquid for photophysical studies. Interestingly, the position of the absorption and emission maximum of C153 remain unchanged after the addition of organic cosolvent to RTIL.

Time-Resolved Studies

The emission decay profile of C153 has been measured at several wavelengths (5–10 nm intervals) across the emission spectra by exciting the sample at 405 nm. The decay profiles are found to be strongly dependent on the monitoring wavelengths (Figure 4). A faster decay is observed when the process is monitored at shorter wavelengths. However, at longer wavelengths, we observed a decay profile that consists of a clear rise with usual decay. This particular observation carries the typical signature of solvation process [38]. The time-resolved emission spectra (TRES) of the system, constructed from the fitted decay profiles, show progressive red shift of the fluorescence maximum with time. Representative TRES of C153 is shown in Figure 5. Time-dependent shifts of the emission maximum to lower energy have been observed in all cases. This indicates that the excited states of dipolar molecules are stabilized by solvent molecules with time.

Table 1: Bond Lengths and Bond Angle in Optimized Structure of [BIMIMDBA][TF₂N] Obtained from B3LYP Functional/6-31++G (d, p) Level Optimization

Systems	Gas phase distances	(Å)	Gas phase bond angles	(°)
[BIMIMDBA][TF ₂ N]	C5-H4	1.081	C14-H17-N28	179.40
	C14-H17	1.083	C14-H17-O33	122.30
	N28-H4	3.034	C5-H4-O34	141.30
	N28-H17	2.451	C14-H17-O34	143.10
	O34-H4	2.172	C14-H4-N28	100.04
	O33-H17	2.614		
	F39-H22	2.726		
	F39-H23	3.825		
	F41-H26	4.585		
	C14-H17-N28	3.833		
	C14-H17-O33	3.800		
	C5-H4-O34	3.800		

Table 2: Absorption and Emission Maxima, Stokes Shift of C153 in Different Systems

System	$\lambda_{\max}(\text{abs})[\text{nm}]$	$\lambda_{\max}(\text{em})[\text{nm}]$	Stokes Shift(cm^{-1})
RTIL+ 0%DMF	442	528	3685
RTIL+6%DMF	442	528	
RTIL+12%DMF	442	528	

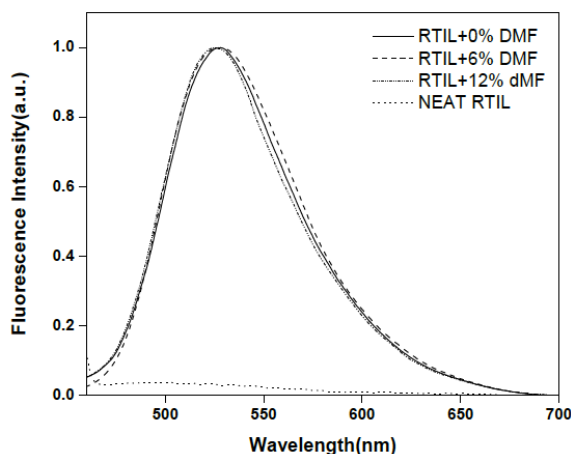


Figure 3: Normalised steady state emission spectrum of C153 in neat RTIL+ DMF mixtures. Emission spectrum of neat RTIL is also shown in the same figure. $\lambda_{\text{exc.}} = 405 \text{ nm}$.

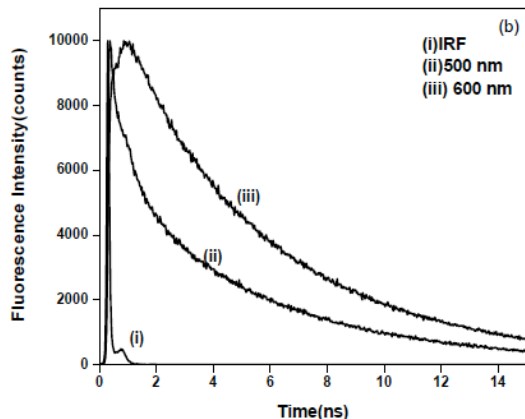
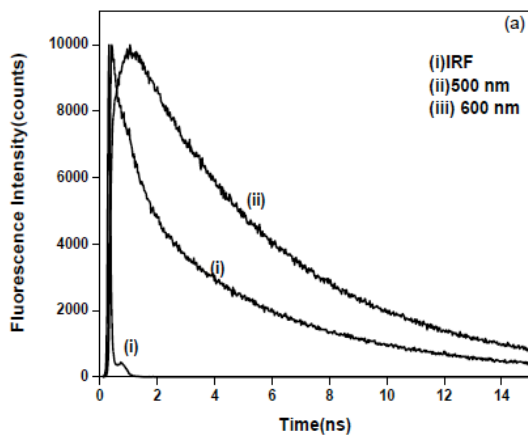


Figure 4: Decay profiles of C153 at different monitoring wavelengths in (a) RTIL+ 6% DMF and in (b) RTIL+12% DMF.

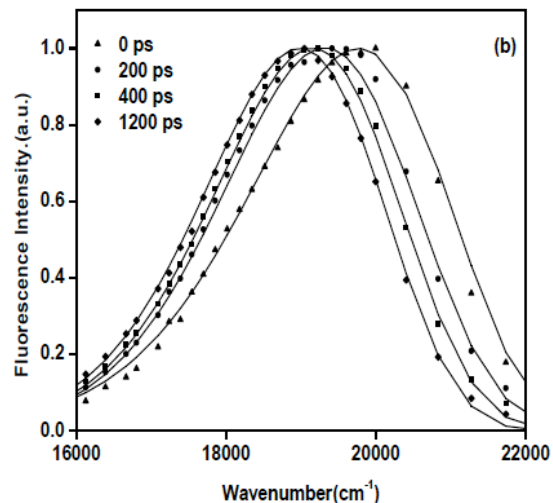
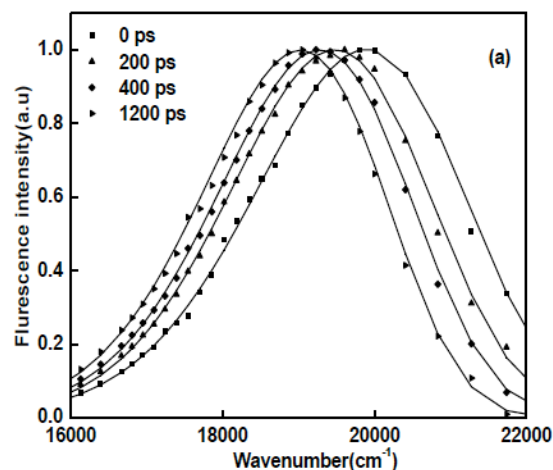


Figure 5: TRES plots C153 in (a) neat RTIL and in (b) RTIL+6wt% DMF mixture.

The total Stokes shift of the fluorescence maximum observed and the relaxation parameters of solvation of C153 for the systems are collected in Table 3. The time constants of the observable dynamics are determined from the plots of the spectral shift correlation function, $C(t)$, versus time. Average solvation time has been calculated by using both bi-exponential function and stretched exponential function. We found that both the fits are providing almost same average solvation time. Decay of solvation correlation function, $C(t)$ of C153 in neat RTIL and RTIL-DMF binary mixtures are shown in the Figure 6.

Table 3: Solvation Relaxation Parameters of C153 in RTIL-DMF Binary Mixtures

Wt% DMF	^a Viscosity(cP)	^b Biexponential Fit					^c Stretched Exponential Fit			^d Observed Shift (cm ⁻¹)
		a ₁	τ ₁ (ns)	a ₂	τ ₂ (ns)	τ _{avg} (ns)	β	τ _{solv}	⟨τ _{st} ⟩(ns)	
0	160	0.57	0.23	0.42	1.11	0.6	0.74	0.47	0.57	1016
6	78	0.64	0.17	0.36	0.84	0.41	0.738	0.317	0.38	855
12	40.7	0.83	0.14	0.18	0.67	0.24	0.841	0.194	0.21	910

^aat 298K, ^bby equation (4), ^cby equation (6), ^dcalculated by $[\bar{\nu}_o - \bar{\nu}_\infty]$

From Table 3, it is evident that the average solvation time of C153 decreases with the increase in wt. percentage of DMF in RTIL. For example, the average solvation time decreases from 600 ps in neat ionic liquid to 240 ps in RTIL-DMF mixture (12 wt%). This lowering of average solvation time with gradual addition of DMF to neat ionic liquid could be attributed to gradual lowering of bulk viscosity of the media. To get a better understanding on the dependence of average solvation time on bulk viscosity of the probe molecule in the different RTIL-DMF composition, we have plotted the average solvation time of C153 against the bulk viscosity values of RTIL-DMF mixtures (Figure 7). Almost a linear decrease in average solvation time with bulk viscosity has been observed. In this context we would like to note that in neat DMF the average solvation and rotational time are found to be 2 ps and 47 ps respectively [43, 44]. The faster dynamics is attributed to the much low viscosity of DMF.

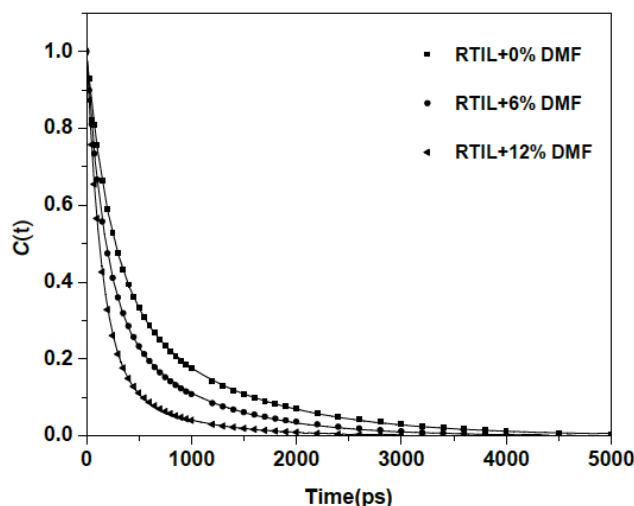


Figure 6: Decay of the spectral shift correlation function, $C(t)$ of C153 in neat RTIL, RTIL+6wt% DMF and RTIL+12wt% DMF ($\lambda_{exc.} = 405$ nm). In all cases, solid lines denote the bi-exponential fit to the data points.

Time-resolved fluorescence anisotropy ($r(t)$) is estimated by the following equation

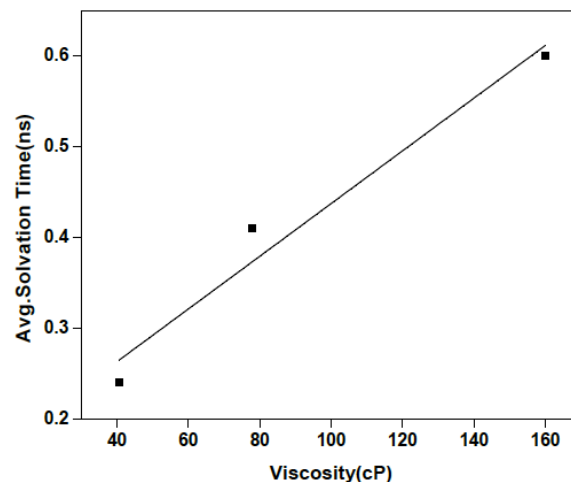


Figure 7: Average solvation time against bulk viscosity at 293 K.

$$r(t) = \frac{G I_{VV}(t) - I_{VH}(t)}{G I_{VV}(t) + 2I_{VH}(t)} \quad \text{Where } G = \frac{\sum I_{HH}(t)}{\sum I_{HV}(t)} \quad (7)$$

where G is the correction factor for detector sensitivity to the polarization of the emission. G is 0.8 at the wavelength of detection. $I_{HH}(t)$ and $I_{HV}(t)$ are the intensities of fluorescence decays when the excitation and the emission polarizers are polarized at horizontal–horizontal and horizontal–vertical alignments respectively. Again $I_{VV}(t)$ and $I_{VH}(t)$ are the intensities of fluorescence decays when excitation and emission polarizers are polarized at vertical–vertical and vertical–horizontal alignments respectively. The rotational relaxation parameters of C153 in neat RTIL and in RTIL-DMF at different temperatures are collected in Table 4. The anisotropy decay profiles are fitted to a bi-exponential function.

Decay of time-resolved anisotropy ($r(t)$) of C153 in RTIL+6%(wt.) DMF at various temperatures are shown in Figure 8.

As can be seen from Table 4, the average rotational time of C153 which is higher in neat ionic liquid

Table 4: Rotational Relaxation Parameters of C153 in RTIL-DMF Binary Mixtures at Different Temperatures ($\lambda_{exc}=405$ nm)

Wt% of DMF in RTIL	Temp.(K)	Viscosity	a_0	a_1	τ_1 (ns)	a_2	τ_2 (ns)	$\langle\tau_r\rangle$ (ns)	${}^b C_{rot}$ (avg.)
0	293	160	0.35	0.17	0.75	0.83	7.69	6.52	0.48
	298	117.4	0.36	0.19	0.47	0.81	5.72	4.74	
	303	88.5	0.35	0.17	0.53	0.82	4.50	3.82	
	308	68.3	0.35	0.18	0.48	0.82	3.52	2.95	
	313	53.5	0.35	0.18	0.31	0.82	2.72	2.29	
6	293	78	0.32	0.22	1.11	0.77	5.37	4.41	0.59
	298	62.3	0.32	0.19	0.83	0.80	3.95	3.35	
	303	50.7	0.30	0.20	0.74	0.80	3.19	2.70	
	308	42.2	0.30	0.18	0.52	0.82	2.40	2.06	
	313	35.8	0.30	0.23	0.72	0.77	2.07	1.75	
12	293	40.7	0.32	0.23	0.85	0.76	3.14	2.6	0.62
	298	32.3	0.32	0.20	0.57	0.80	2.36	2.00	
	303	26	0.38	0.27	0.09	0.72	1.68	1.24	
	308	23.5	0.35	0.20	0.13	0.80	1.41	1.15	
	313	19.7	0.36	0.20	0.13	0.80	1.17	0.95	

${}^a r_0$ is the initial anisotropy.

${}^b C_{rot}$ is rotational coupling constant calculated according to equation 11. Temperature averaged C_{rot} values are tabulated.

gradually decreases with gradual addition of DMF to RTIL. For example, at 293 K, the average rotational time of C153 decreases from 6.52 ns in neat ionic liquid to 2.60 ns in RTIL-DMF (12wt %) mixture. The faster rotation of C153 with decrease in viscosity of the RTIL-DMF mixture is also evident when the average rotational time of C153 is plotted against the viscosity of the media. The log-log plot of average rotational relaxation time (τ_r) against viscosity with respect to temperature is shown in Figure 9. It is clear from the plot that rotational relaxation dynamics of C153 can be well explained within the broad limits of SED hydrodynamic theory. It is also evident from the plot that the average rotational relaxation time decreases with lowering of the bulk viscosity of the media. We have also fitted the $\langle\tau_r\rangle$ and η/T data for C153 to the function, $\tau_r = A(\eta/T)^P$. In these expressions (equations 8, 9 and 10), the τ_r values are in nanoseconds and η/T are in cPK^{-1} , and N and R denote the number of data points and regression coefficient, respectively. Prominent nonlinear composition dependence has not been observed in the present case (equations 8, 9 and 10).

C153 in RTIL+ 0(wt%)DMF

$$\langle\tau_r\rangle = (11.203 \pm 0.2913) (\eta/T)^{0.887 \pm 0.02584} \quad (N=5, R=0.9988) \quad (8)$$

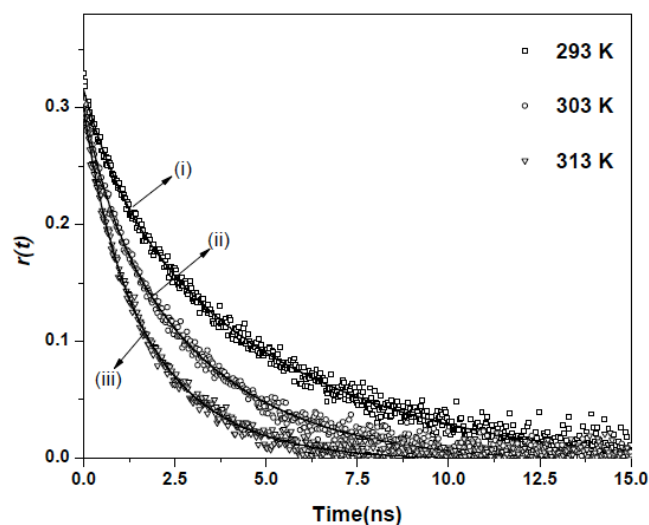


Figure 8: Decay of time-resolved anisotropy ($r(t)$) of C153 in RTIL+6%(wt.) DMF at $\lambda_{exc} = 405$ nm at temperatures (i) 293 K, (ii) 303 K and (iii) 313 K respectively. Solid line represents biexponential fitting to the data points.

C153 in RTIL+ 6(wt%)DMF

$$\langle\tau_r\rangle = (18.704 \pm 0.7959) (\eta/T)^{1.069 \pm 0.026} \quad (N=5, R=0.9991) \quad (9)$$

C153 in RTIL+ 12(wt%)DMF

$$\langle\tau_r\rangle = (32.9689 \pm 13.62) (\eta/T)^{1.28 \pm 0.185} \quad (N=5, R=0.9712) \quad (10)$$

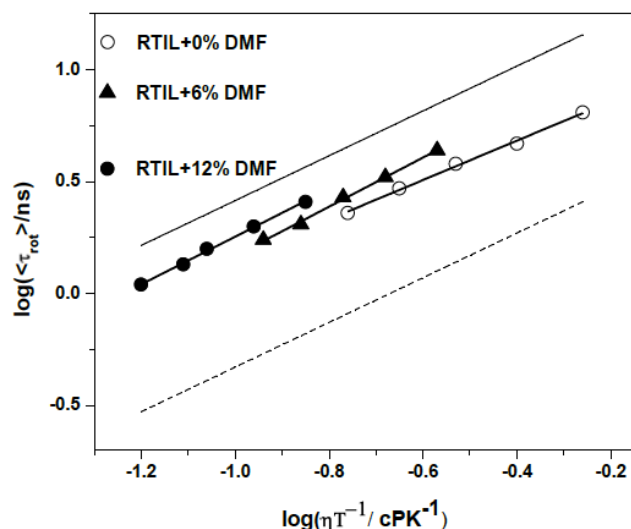


Figure 9: The log-log plots of $\langle \tau_{rot} \rangle$ Vs. (η/T) showing the stick and slip boundary conditions with solid and dashed line respectively.

We have also estimated the rotational coupling constants (C_{rot}) of C153 at different RTIL-DMF composition. According to the stick hydrodynamic theory, the rotational time constant (τ_{stk}) of a nonspherical solute of volume V , rotating along the axis of the ellipsoid in a medium of viscosity η at temperature T is given by

$$\tau_{stk} = V f_{stk} \eta / k_B T \quad (11)$$

where f_{stk} accounts for nonspherical shape of the solute and k_B is the Boltzmann constant. Using the literature value of $V(243 \text{ \AA}^3)$ and $f_{stk}(1.5)$, we computed the τ_{stk} values for RTIL and RTIL-DMF mixture [7]. From the computed τ_{stk} values, the rotational coupling constants, C_{rot} , which is defined as $C_{rot} = \tau_{rot} / \tau_{stk}$, is calculated. As can be seen from Table 4, the C_{rot} value varies from 0.48 to 0.62. The calculated C_{rot} values, which are measure of the extent of departure from normal hydrodynamic behavior of a solute due to specific interaction, are found to be very similar to that obtained for C153 in conventional solvents [44]. The calculated C_{rot} values also indicate no involvement of specific solute-solvent interaction in the present case. The observation demonstrates that other than the lowering of viscosity of the medium, DMF does not seem to play any role towards the rotational dynamics of C153 in RTIL-DMF mixtures.

CONCLUSION

We have studied the steady state and time resolved fluorescence behavior of C153 in a new diimidazolium cation based ionic liquid and its mixture with organic

polar cosolvent DMF to determine the role of DMF that it plays in governing the solvation and rotational relaxation of C153 in these media. The present ionic liquid has negligible emission behavior and so is well suited for fluorescence studies. Steady state spectral behavior of C153 is found not to be affected by these polar cosolvents. However, in time-resolved fluorescence studies the influence of DMF is clearly observed. The addition of DMF to RTIL decreases the average solvation time due to a lowering of viscosity of the media. This also results in the faster rotational dynamics of C153.

ACKNOWLEDGEMENT

MS is thankful to Department of Science and Technology (DST), Government of India, for a research grant. PKS thanks National Institute of Science Education and research (NISER) and SKD thanks Council of Scientific and Industrial Research (CSIR) for the fellowship.

REFERENCES

- [1] Wasserscheid P, Keim W. Ionic liquids: New "solutions" for transition metal catalysis. *Angew Chem Int Ed* 2000; 39: 3772-89. [http://dx.doi.org/10.1002/1521-3773\(20001103\)39:21<3772::AID-ANIE3772>3.0.CO;2-5](http://dx.doi.org/10.1002/1521-3773(20001103)39:21<3772::AID-ANIE3772>3.0.CO;2-5)
- [2] Rogers RD, Seddon KR. Ionic Liquids-Solvents of the future? *Science* 2003; 302: 792-3. <http://dx.doi.org/10.1126/science.1090313>
- [3] Köddermann T, Wertz C, Heintz A, Ludwig R. The association of water in ionic liquids: A reliable measure of polarity. *Angew Chem Int Ed* 2006; 45: 3697-70. <http://dx.doi.org/10.1002/anie.200504471>
- [4] Samanta A. Dynamic Stokes shift and excitation wavelength dependent fluorescence of dipolar molecules in room temperature ionic liquids. *J Phys Chem B* 2006; 110: 13704-6. <http://dx.doi.org/10.1021/jp060441q>
- [5] Samanta A. Solvation dynamics in ionic liquids: What we have learned from the dynamic fluorescence Stokes shift studies. *J Phys Chem Lett* 2010; 1(10): 1557-62. <http://dx.doi.org/10.1021/jz100273b>
- [6] Paul A, Samanta A. Effect of nonpolar solvents on the solute rotation and solvation dynamics in an imidazolium ionic liquid. *J Phys Chem B* 2008; 112: 947-53. <http://dx.doi.org/10.1021/jp077536s>
- [7] Ito N, Arzhantsev S, Maroncelli M. The probe dependence of solvation dynamics and rotation in the ionic liquid 1-butyl-3-methyl-imidazolium hexafluorophosphate. *Chem Phys Lett* 2004; 396: 83-91. <http://dx.doi.org/10.1016/j.cplett.2004.08.018>
- [8] Chakrabarty D, Chakraborty D, Seth D, Hazra P, Sarkar N. Dynamics of solvation and rotational relaxation of Coumarin 153 in 1-butyl-3-methylimidazolium hexafluorophosphate [bmim][PF₆]-water mixtures. *Chem Phys Lett* 2004; 397: 469-74. <http://dx.doi.org/10.1016/j.cplett.2004.08.141>
- [9] Chakrabarty D, Chakraborty D, Seth D, Hazra P, Sarkar N. Effect of Water, Methanol, and Acetonitrile on Solvent

- Relaxation and Rotational Relaxation of Coumarin 153 in Neat 1-Hexyl-3-methylimidazolium Hexafluorophosphate. *J Phys Chem A* 2005; 109: 1764-69.
<http://dx.doi.org/10.1021/jp0460339>
- [10] Pramanik R, Rao VG, Sarkar S, Ghatak C, Setua P, Sarkar N. To probe the interaction of methanol and acetonitrile with the ionic liquid *N,N,N*-Trimethyl-*N*-propyl ammonium Bis(trifluoromethanesulfonyl) imide at different temperatures by solvation dynamics study. *J Phys Chem B* 2009; 113: 8626-34.
<http://dx.doi.org/10.1021/jp900627h>
- [11] Sarkar S, Pramanik R, Ghatak C, Setua P, Sarkar N. Probing the interaction of 1-Ethyl-3-methylimidazolium Ethyl Sulfate ([Emim][EtSO₄]) with alcohols and water by solvent and rotational relaxation. *J Phys Chem B* 2010; 114: 2779-89.
<http://dx.doi.org/10.1021/jp907936s>
- [12] Daschakraborty S, Biswas R. Stokes shift dynamics in (ionic liquid + polar solvent) binary mixtures: Composition dependence. *J Phys Chem B* 2011; 115: 4011-24.
<http://dx.doi.org/10.1021/jp200407m>
- [13] Das SK, Sarkar M. Steady-state and time-resolved fluorescence behavior of coumarin-153 in a hydrophobic ionic liquid and ionic liquid-toluene mixture. *J Mol Liq* 2012; 165: 38-43.
<http://dx.doi.org/10.1016/j.molliq.2011.10.004>
- [14] Gutowski KE, Broker GA, Willauer HD, *et al.* Controlling the aqueous miscibility of ionic liquids: Aqueous biphasic systems of water-miscible ionic liquids and water-structuring salts for recycle, metathesis, and separations. *J Am Chem Soc* 2003; 125: 6632-3.
<http://dx.doi.org/10.1021/ja035180z>
- [15] Dupont J, de Souza RF, Suarez PAZ. Ionic liquid (molten salt) phase organometallic catalysis. *Chem Rev* 2002; 102: 3667-92.
<http://dx.doi.org/10.1021/cr010338r>
- [16] GZ Wu, Liu YD, Long DW. Effect of ionic liquid [Me₃NC₂H₄OH]⁺ [ZnCl₄]⁻ on γ - radiation polymerization of methylmethacrylate in ethanol and *N,N*-Dimethylformamide. *Macromol Rapid Commun* 2005; 26: 57-9.
<http://dx.doi.org/10.1002/marc.200400375>
- [17] Dai S, Ju YH, Barnes CE. Solvent extraction of strontium nitrate by a crown ether using room-temperature ionic liquids. *Dalton Trans* 1999; 1201-2.
- [18] Visser AE, Swatoski RP, Reichert WM, Griffin ST, Rogers RD. Traditional extractants in nontraditional solvents: Groups 1 and 2 extraction by crown ethers in room-temperature ionic liquids. *Ind Eng Chem Res* 2000; 29: 3596-604.
<http://dx.doi.org/10.1021/ie000426m>
- [19] Widegen JA, Laesecke A, Magee JW. The effect of dissolved water on the viscosities of hydrophobic room temperature ionic liquids. *Chem Commun* 2005; 1610-2.
<http://dx.doi.org/10.1039/b417348a>
- [20] Fletcher KA, Pandey S. Solvatochromic probe behavior within ternary room-temperature ionic liquid 1-Butyl-3-methylimidazolium Hexafluorophosphate + ethanol + water solutions. *J Phys Chem B* 2003; 107: 13532-9.
<http://dx.doi.org/10.1021/jp0276754>
- [21] Baker SN, Baker GA, Bright FV. Temperature-dependent microscopic solvent properties of 'dry' and 'wet' 1-butyl-3-methylimidazolium hexafluorophosphate: correlation with $E_T(30)$ and Kamlet-Taft polarity scales. *Green Chem* 2002; 4: 165-9.
<http://dx.doi.org/10.1039/b111285f>
- [22] Fletcher KA, Pandey S. Solvatochromic probe behavior within binary room-temperature ionic liquid 1-Butyl-3-methylimidazolium Hexafluorophosphate plus ethanol solutions. *Appl Spectrosc* 2002; 56: 1498-504.
<http://dx.doi.org/10.1366/00037020260377823>
- [23] Harifi-Mood AR, Habibi-Yangjeh A, Gholami MR. Solvatochromic parameters for binary mixtures of 1-(1-Butyl)-3-methylimidazolium Tetrafluoroborate with some protic molecular solvents. *J Phys Chem B* 2006; 110: 7073-8.
<http://dx.doi.org/10.1021/jp0602373>
- [24] Mellein BR, Aki SNVK, Ladewski RL, Brennecke JF. Effect of water and organic solvents on the ionic dissociation of ionic liquids. *J Phys Chem B* 2007; 111: 6452-6.
<http://dx.doi.org/10.1021/jp071051m>
- [25] Jarosik A, Krajewski SR, Lewandowski A, Radzinski P. Conductivity of ionic liquids in mixtures. *J Mol Liq* 2006; 123: 43-50.
<http://dx.doi.org/10.1016/j.molliq.2005.06.001>
- [26] Tokuda H, Baek SJ, Watanabe M. Room-temperature ionic liquid-organic solvent mixture: Conductivity and ion association. *Electrochemistry* 2005; 73: 620-2.
- [27] Žagar E, Žigon M. Solution properties of carboxylated polyurethanes and related ionomers in polar solvents (DMF and LiBr/DMF). *Polymer* 2000; 41: 3513-21.
[http://dx.doi.org/10.1016/S0032-3861\(99\)00604-7](http://dx.doi.org/10.1016/S0032-3861(99)00604-7)
- [28] Kang YK, Park HS. Internal rotation about the C-N bond of amides. *J Mol Struct (Theochem)* 2004; 676: 171-6.
<http://dx.doi.org/10.1016/j.theochem.2004.01.024>
- [29] Borrmann H, Persson I, Sandström M, Stålhandske CMV. The crystal and liquid structures of *N,N*-dimethylthioformamide and *N,N*-dimethylformamide showing a stronger hydrogen bonding effect for C-H...S than for C-H...O. *J Chem Soc Perkin Trans 2* 2000; 393-402.
<http://dx.doi.org/10.1039/a904531g>
- [30] Umebayashi Y, Matsumoto K, Watanabe M, Ishiguro S. Individual solvation number of first-row transition metal(II) ions in solvent mixtures of *N,N*-dimethylformamide and *N,N*-dimethylacetamide-Solvation steric effect. *Phys Chem Chem Phys* 2001; 3: 5475-81.
<http://dx.doi.org/10.1039/b107342g>
- [31] García B, Alcalde R, Leal JM, Matos JS. Shear viscosities of the *N*-methylformamide- and *N,N*-dimethylformamide-(C₁ - C₁₀) alkan-1-ol solvent systems. *J Chem Soc Faraday Trans* 1997; 93: 1115-8.
<http://dx.doi.org/10.1039/a607876a>
- [32] Venkatesu P, Lee MJ, Lin HM. Volumetric properties of (*N,N*-dimethylformamide + aliphatic diethers) at temperatures ranging from (298.15 to 358.15) K. *J Chem Thermodyn* 2005; 53: 996-1002.
<http://dx.doi.org/10.1016/j.jct.2005.01.002>
- [33] Attri P, Reddy PM, Venkatesu P, Kumar A, Hofman T. Measurements and molecular interactions for *N,N*-Dimethylformamide with ionic liquid mixed solvents. *J Phys Chem B* 2010; 114: 6126-33.
<http://dx.doi.org/10.1021/jp101209j>
- [34] Sturlaugson AL, Fruchey KS, Fayer MD. Orientational dynamics of room temperature ionic liquid/water mixtures: Water-induced structure. *J Phys Chem B* 2012; 116: 1777-87.
<http://dx.doi.org/10.1021/jp209942r>
- [35] Jiang W, Wang Y, Voth GA. Molecular dynamics simulation of nanostructural organization in ionic liquid/water mixtures. *J Phys Chem B* 2007; 111: 4812-8.
<http://dx.doi.org/10.1021/jp067142j>
- [36] Roth C, Appelhagen A, Jobst N, Ludwig R. Microheterogeneities in ionic-liquid-methanol solutions studied by FTIR Spectroscopy, DFT Calculations and molecular dynamics simulations. *Chem Phys Chem* 2012; 13: 1708-17.
<http://dx.doi.org/10.1002/cphc.201101022>
- [37] Raabe G, Köhler J. Thermodynamical and structural properties of binary mixtures of imidazolium chloride ionic liquids and alcohols from molecular simulation. *J Chem Phys* 2012; 129: 144503-8.
<http://dx.doi.org/10.1063/1.2990653>

- [38] Maroncelli M, Fleming GR. Picosecond solvation dynamics of coumarin 153: The importance of molecular aspects of solvation. *J Chem Phys* 1987; 86: 6221-39. <http://dx.doi.org/10.1063/1.452460>
- [39] Becke DA, Density-functional thermochemistry. III. The role of exact exchange. *J Chem Phys* 1993; 98: 5648-52. <http://dx.doi.org/10.1063/1.464913>
- [40] Lee C, Yang W, Parr RG. Development of the Colic-Salvetti correlation-energy formula into a functional of the electron density. *Phys Rev B* 1988; 37: 785-9. <http://dx.doi.org/10.1103/PhysRevB.37.785>
- [41] Frisch MJ, Trucks GW, Schlegel HB, Scuseria GE, Robb MA, Cheeseman JR, Zakrzewski VG, Montgomery JA, Stratmann RE Jr, Burant JC, Dapprich S, Millam JM, Daniels AD, Kudin KN, Strain MC, Farkas O, Tomasi J, Barone V, Cossi M, Cammi R, Mennucci B, Pomelli C, Adamo C, Clifford S, Ochterski J, Petersson GA, Ayala PY, Cui Q, Morokuma K, Malick DK, Rabuck AD, Raghavachari K, Foresman JB, Cioslowski J, Ortiz JV, Stefanov BB, Liu G, Liashenko A, Piskorz P, Komaromi I, Gomperts R, Martin RL, Fox DJ, Keith T, Al Laham MA, Peng Y, Nanayakkara CA, Gonzalez C, Challacombe M, Gill PMW, Johnson B, Chen W, Wong MW, Andres JL, Gonzalez C, Head-Gordon M, Replogle ES, Pople JA, Gaussian 03; Revision C.02: Gaussian, Inc.: Wallingford, CT 2004.
- [42] Rahim Z, Barman BN, *Acta Crystallographica A* 1978; 34: 761-4. <http://dx.doi.org/10.1107/S0567739478001576>
- [43] Horng ML, Gardecki J, Papazyan A, Maroncelli M. Subpicosecond measurements of polar solvation dynamics: Coumarin 153 revisited. *J Phys Chem* 1995; 99: 17311-37. <http://dx.doi.org/10.1021/j100048a004>
- [44] Horng ML, Gardecki J, Maroncelli M. Rotational dynamics of Coumarin 153: Time-dependent friction, dielectric friction, and other nonhydrodynamic effects. *J Phys Chem A* 1997; 101: 1030-47. <http://dx.doi.org/10.1021/jp962921v>

Received on 20-11-2012

Accepted on 07-02-2013

Published on 28-02-2013

DOI: <http://dx.doi.org/10.6000/1929-5030.2013.02.01.6>